SCIENCE CHINA
Technological Sciences

Special Issue: Celebrating the 100th Anniversary of Harbin Institute of Technology
•Review•

August 2020 Vol.63 No.8: 1335–1347
https://doi.org/10.1007/s11431-020-1665-3

A review of high frequency resonant DC-DC power converters: Topologies and planar magnetic technologies

XU DianGuo, GUAN YueShi*, WANG YiJie & WANG Wei

School of Electrical Engineering and Automation, Harbin Institute of Technology, Harbin 150001, China

Received March 5, 2020; accepted June 2, 2020; published online July 17, 2020

With the development of high frequency resonant DC-DC power converters, the system efficiency, power density and dynamic characteristics have been significantly improved. High frequency resonant DC-DC converters have been applied in DC grid, renewable energy, transportation, aerospace, point-of-load (POL) power supply and many other fields. Under high switching frequencies, switching loss and magnetic loss are the main concerns; thus, the resonant topology and planar magnetic are two key technologies to reduce loss. This review compares different resonant topologies and analyzes the advantages and disadvantages respectively, such as LLC circuit, dual active bridge (DAB) circuit, and other high order resonant circuits. For planar magnetic components, optimal winding structures, modeling methods and integration methods are thoroughly surveyed. With corresponding topics, the opportunities and challenges in the future development are summarized, which mainly focus on the characteristics of wide bandgap devices, such as the dynamic resistance, output capacitance loss and also the integrated module. This review can be a helpful guidance when designing high frequency resonant DC-DC converters.

high frequency, resonant DC-DC power converter, planar magnetic components

Citation: Xu D G, Guan Y S, Wang Y J, et al. A review of high frequency resonant DC-DC power converters: Topologies and planar magnetic technologies. Sci China Tech Sci, 2020, 63: 1335–1347, https://doi.org/10.1007/s11431-020-1665-3

1 Introduction

In the recent years, there is an urgent need of high efficiency and high power density for DC-DC power converters. For DC-DC power converters, magnetic and capacitive components occupy most of the space, which can be greatly shrunk by increasing switching frequencies. With the maturity of wide bandgap devices, the operating frequencies of DC-DC power converters have been increased to hundreds of kHz and even several MHz. However, one major concern is that the switching loss significantly increases with the increment of operating frequencies. Thus, soft-switching technology is widely adopted to reduce switching loss, where resonant converters are the most important and widely used methods to achieve soft-switching and reduce switching loss. Thus, high frequency resonant DC-DC converters have been applied in DC grid, renewable energy, transportation, aerospace, POL power supply, battery charger, energy storage system and many other fields [1–8].

For example, the power consumption of data centers has increased rapidly. At the same time, the increasing number of servers also causes the data center occupying more and more space. Therefore, how to improve the efficiency and reduce the volume have become the main bottlenecks for the development of data centers. For this application, many high frequency resonant DC-DC converters dealing with different voltage level conversion are developed, such as 400 to 48 V, 400 to 12 V and even 48 to 1 V. The development of high frequency resonant converters can provide a strong guarantee for energy and space-intensive data centers [9–11].

Also, compared with low frequency converters, one sig-

*Corresponding author (email: hitguanyueshi@163.com)

nificant difference of high frequency resonant converters is that the magnetic components can be realized by planar structure. The large number of wounded litz winding can be replaced by small number of copper track winding on PCB. For planar magnetic components, the winding structure can be more flexible and the component consistency can be improved. For magnetic components, the core loss and copper (winding) loss increases rapidly with the increment of switching frequencies. On one hand, the core loss can be reduced by adopting low loss density and low permeability material. Also, the integration of several magnetic cores can reduce the number of core and corresponding loss. On the other hand, optimizing the winding layout to reduce its DC and AC resistance under high frequency conditions is a difficult and important issue. What is more, different from the traditional winding structures, its disadvantage is that once the PCB is manufactured, the winding structure cannot be flexibly adjusted. Therefore, under high-frequency operating conditions, efficient and accurate design methods of magnetic components are gradually proposed [12–15].

The fast development of high frequency resonant DC-DC converters is also based on the development of semiconductor devices. Though Si semiconductor device technology is still progressing, its on-resistance and input/output capacitance characteristics have basically reached their limits. With the continuous development of new wide bandgap (WBG) semiconductor such as GaN and SiC, the performance of WBG devices has been greatly improved, further reducing the switching losses. However, some unique characteristics are different from traditional Si devices, which need to be paid attention to. For example, compared with traditional Si switches, GaN FETs have no reverse recovery loss, but there is higher reverse conduction loss. Therefore, in the design process of high-frequency resonant DC-DC converters, it is necessary to comprehensively consider the influence between device, topology and other aspects in order to achieve a comprehensive improvement in its efficiency and power density. Meanwhile, some unexplained phenomenon and characteristics, such as dynamic resistance and output capacitance loss need to be further investigated. They greatly affect the topology selection and parameter design [16–19].

In the review, topologies and planar magnetic technologies of high frequency resonant DC-DC converters are surveyed. Sect. 2 describes the topologies of high frequency resonant DC-DC converters, also the operating modes and characteristics are depicted. Sect. 3 analyzes the application of planar magnetic components in high frequency resonant DC-DC converters, including optimal winding structures, modeling methods and integration methods. Sect. 4 points out the opportunities and challenges in the future development. Finally, Sect. 5 concludes this paper.

2 Topology of high frequency resonant converters

2.1 LLC resonant converters

The resonant converters are widely preferred in high frequency applications to solve high switching loss caused by the increment of switching frequencies. LLC circuit, the most typical series-parallel resonant circuit, is shown in Figure 1, which has been widely adopted in many applications.

The most attractive characteristic of the LLC resonant converter is that all the switches in primary side can achieve zero voltage switching (ZVS), and the secondary-side diode or synchronous rectification (SR) MOSFET can also achieve zero current switching (ZCS) when the converter operates at or below the resonant frequency [20–23]. Therefore, LLC converter is one of the most commonly used high frequency converters. Though the design and control process of LLC are quite mature, when applied to high frequency applications and combined with the WBG semiconductor devices, some new challenges appear.

With the continuous development of high frequency technique, parameter design of LLC converters needs to be adjusted. Ref. [24] analyzes the benefits of GaN devices in a 300 W, 1 MHz LLC resonant converter, comparing with Si-based converter, where 24.8% loss reduction is achieved, and the full-load efficiency is up to 96.6%. However, under high switching frequency condition, ZVS failure cannot be predicted accurately by only considering traditional constraints. To solve this problem, ref. [25] investigates the failure mode of LLC in detail and an accurate ZVS boundary is proposed for high frequency design. At the same time, in high frequency applications, the power stage design must take secondary leakage inductance into account because it affects the voltage gain. Ref. [26] proposes a modified LLC resonant converter model that incorporates the secondary leakage inductance for more accurate analysis.

Besides the efficiency under rated output condition, the light-load efficiency has drawn more and more attention for LLC resonant converters. However, because of the higher load-independent loss and difficulties in high-frequency control, the light-load efficiency improvement for high-fre-

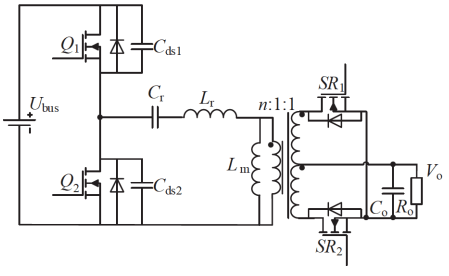

Figure 1 Schematic circuit of LLC converter.

quency LLC converter is even more challenging.

To improve system efficiency at low voltage and light-load conditions, ref. [27] proposes a hybrid LLC resonant converter as shown in Figure 2. The converter is switched among three different operation modes, namely full-bridge converter, dual-phase half-bridge LLC converter and single-phase half-bridge LLC converter. By changing the switching frequency, the transitions can be formed smoothly and stably among three modes, without using additional switches. The proposed theory is verified on a 3.2 kW prototype using GaN devices with the power density of 65 W cm^{-3}. Experimental results show that the proposed converter has a peak efficiency of 98.5% at full load condition with an improvement efficiency about 1% at low-voltage and 2.3% under light-load conditions, compared to the conventional full-bridge LLC converter.

However, the method of pulse frequency modulation to improve the efficiency is limited due to the load-independent loss. Ref. [28] states that burst mode is an effective way to improve the light-load efficiency. Because of the dynamics of the resonant tank, the conventional burst mode control has limited efficiency improvement of LLC converter. Ref. [29] proposes an optimal trajectory control (OTC) for burst mode of LLC converter to optimize burst mode efficiency. But the implementation of OTC for burst mode requires high-performance FPGA controller and complex analog circuitry, which is not feasible for industrial applications. Ref. [30] mentions that based on the concept of the simplified OTC (SOTC), the control of the LLC converters with cost-effective MCUs attracts widespread attention and different SOTC control functions have been integrated in a cost-effective MCU. The control scheme of SOTC is shown in Figure 3.

In ref. [31], different SOTC control functions have been integrated in a cost-effective MCU and demonstrated on a 130-kHz LLC converter. Experimental results show that, in light-load efficiency condition, burst-mode with fixed three-pulse switching pattern is superior to other burst-mode control methods, but it still has limitations for high-frequency LLC converters with low-cost MCUs. Ref. [32] proposes a SOTC for adaptive burst mode of high-frequency LLC converters to overcome the limitation caused by the increased impact of digital delay in high-frequency operation. The switching pulse number during burst-on time increases as the load increases and the LLC converter can still operate at the peak-efficiency condition. The proposed method can achieve fast transient response and significant light-load efficiency improvement.

In terms of closed loop control, the conventional digital controller is limited in some high frequency applications, because of its limited frequency resolution which can induce high primary-side and secondary-side current variation and lead to poor output voltage regulation. Ref. [33] proposes a hybrid control method combining pulse frequency modulation (PFM) and pulse width modulation (PWM) to overcome the control performance degradation caused by the limited frequency resolution of the general-purpose DSP at high switching frequency operation. The proposed hybrid control method can enhance the output voltage regulation performance in the steady-state operation using two independent control variables, the pulse width and the switching frequency. Figure 4 shows the output voltage regulation mechanism and control flowchart of the hybrid control algorithm. In the proposed hybrid control method, a PWM control block and a control mode selection block are added on the basis of conventional PFM control to minimize the steady-state error in the output voltage. By determining the priority between two independent control variables at a specific operating point, the combination of PWM and PFM control in the hybrid control method can be implemented. The proposed theory is verified on a 1 MHz, 240 W prototype, and the proposed control method reduces the peak current by 93% and 90% in the primary and secondary sides, respectively, and reduces the output voltage ripple by 68%.

The SRs are critical for the LLC converters to improve the efficiency by reducing the conduction loss of diode rectifiers. However, SR driving schemes are quite challenging under high frequency because of the discrepancy between the primary driving signal and the SR driving signal. Some SR driving schemes have been suggested, such as using a linear compensator and using an independent driving circuit. But these schemes have limitations which can only be applied in

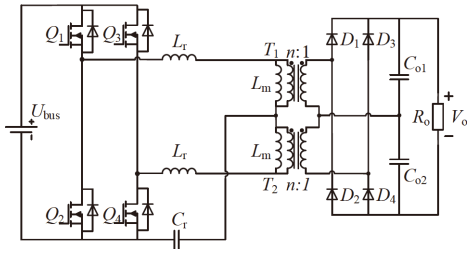

Figure 2 Schematic circuit of the proposed hybrid LLC converter.

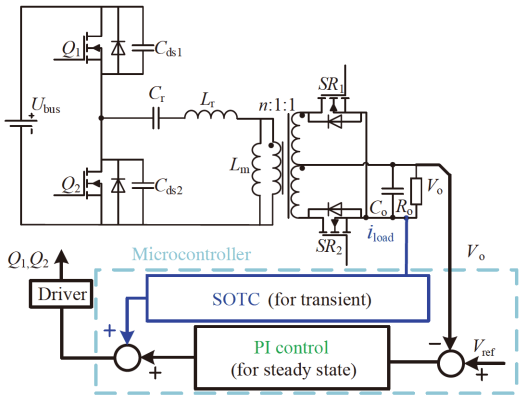

Figure 3 (Color online) One control scheme of SOTC.

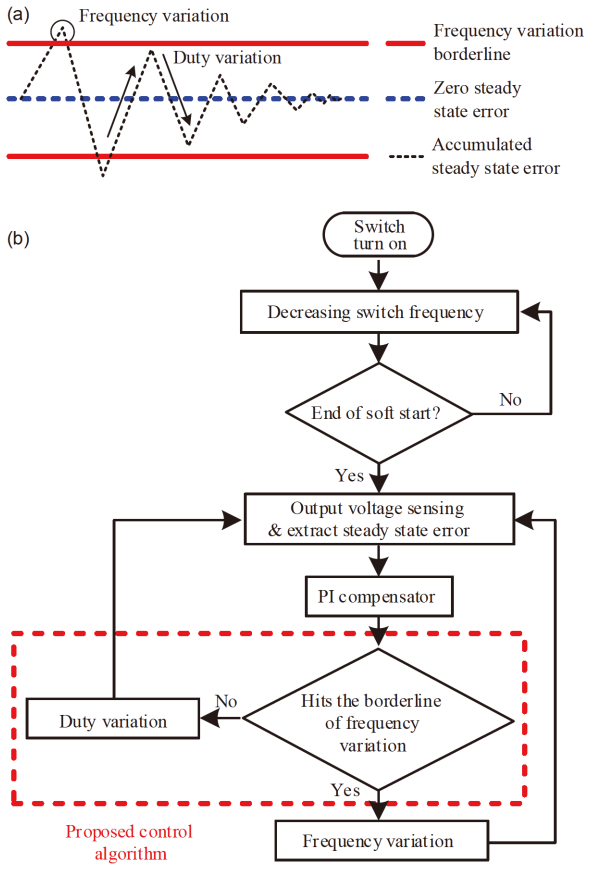

Figure 4 (Color online) PWM and PFM hybrid control algorithm. (a) Output voltage regulation mechanism; (b) control flowchart.

specific situations [34]. Ref. [35] proposes a digital implementation of adaptive SR driving scheme for high-frequency LLC converters with cost-effective microcontroller, as shown in Figure 5. Compared with the other SR driving schemes, the proposed method is suitable to be embedded into digital controller, while at the same time, minimizing the CPU utilization and extra components. The proposed SR driving scheme detects body diode conduction by sensing SR drain-source voltage, and tune the SR on-time every several switching cycles using ripple (asynchronous) counter to minimize body diode conduction loss.

Recently, LLC converters applied in high power and wide output voltage range situations are very important and widely used. To deal with the wide output power range problem, a full bridge LLC resonant converter for EV battery charger is proposed in ref. [36], in which the output power is 10 kW and the output voltage range is from 250 to 450 V. The system efficiency can be as high as 97% based on optimal parameter design. For wide output voltage, an optimal design method of LLC circuit is also proposed based on simplified operation mode analysis [37]. The output voltage range is from 300 to 600 V and the highest efficiency is about 96% under 1 kW output power. Besides optimal parameter design, some modified topologies and control strategies have been

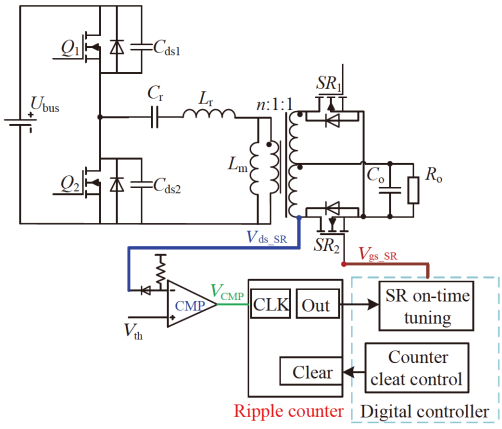

Figure 5 (Color online) Integrated adaptive SR driving for high-frequency LLC converters.

proposed. In ref. [38], a novel pulse width modulated LLC resonant converter based on voltage quadrupler rectifier is proposed, which can always operate at the optimal resonant frequency. The output voltage is from 250 to 420 V and the highest efficiency is about 94%. In ref. [39], the LLC converter is integrated with a phase-shift topology, in which all the switches can achieve ZVS turn-on characteristics and operate at a constant frequency. The output voltage can vary from 200 to 680 V. A 20 kW off-board charger based on LLC circuit is described in ref. [40]. The output voltage is from 300 to 570 V. A interleaved secondary side is used in the LLC circuit, and the highest efficiency is about 98.3%. Though the efficiencies of LLC circuits have been improved based abovementioned methods, however, the efficiencies under the high output voltage or low output voltage conditions are still much lower than the rated situation. Thus, for wide output voltage range LLC converters, there is still great challenge to reduce the effect of large voltage variation.

To further improve both efficiency and power density, further efforts need to be spent on the design, optimization, and magnetic integration of transformers. Ref. [41] states that the matrix transformer can help to increase the output current capability by distributing the secondary current with multiple cores. Ref. [42] proposes the concept of flux cancelation to reduce core size and loss. But it has large distributed inter winding capacitance and large common mode (CM) noise current for high input voltage applications. To solve this problem, ref. [43] uses four-layer PCB windings and places two shielding layers between primary and secondary windings. Therefore, the CM noise current can only circulate in the primary side. The proposed theory is verified on a 380 V/12 V LLC converter with a design optimization procedure and the peak efficiency is around 97%. However, these designs still have the problems of complex structure and multiple cores, so the efficiency can be further improved.

Ref. [44] proposes a novel matrix transformer structure,

integrating four elemental transformers into one magnetic core and utilizing a simple four-layer PCB as the windings, to overcome the challenge of multiple cores. The proposed design scheme can reduce core loss by eliminating and reducing magnetic flux density. The SRs and output capacitance are integrated into the secondary winding to reduce leakage and terminal loss. Compared with the most advanced matrix transformer technology, the core loss of the proposed matrix transformer is reduced by more than half. The proposed theory is verified on a 1 MHz, 800 W LLC prototype with GaN devices and the proposed matrix transformer structure. The prototype fits in quarter-brick footprint, achieves a peak efficiency of 97.6% and a power density of 900 W/inch^3.

2.2 DAB resonant converters

In recent years, bidirectional isolated converters under high frequency conditions have attracted extensive attention in medium-voltage power conversion systems, energy storage systems and solid state transformer (SST). The dual active bridge (DAB) DC-DC converter has become a research hotspot due to its advantages of symmetrical structure, large transmission power capacity and easy soft-switching characteristics [45,46]. Figure 6 shows the circuit diagram of the DAB converter topology. It has two H-bridges, primary-bridge and secondary-bridge. Studies on DAB mainly focus on the following aspects: control strategy, design of soft-switching, and hardware optimization.

DAB converters generally adopt phase shift control, including single-phase-shift (SPS), extended-phase-shift (EPS), dual-phase-shift (DPS) and triple-phase-shift (TPS). These four basic control methods are shown in Figure 7 [47]. SPS control is the most widely used algorithm which is simple and easy for feedback adjustment. In primary H bridge and secondary H bridge, the output voltages of leg middle-points are square waveform with 0.5 duty cycle. Phase is shifted between primary and secondary side to regular output voltage as Figure 7(a) shown. There is one control degree D. However, it can only control the output power of the system by adjusting a single variable, and cannot adjust the characteristics of the system such as reactive power and current stress. To solve this problem, other control methods with more control degree are proposed. For EPS, an inner phase-shift is added between the two bridges in primary H bridge as Figure 7(b) shown. Then, the output voltage of leg middle-point is a three-level waveform, within the time of zero voltage level, the circulating current and power is reduced. There are two control degrees D_1 and D_2. As a controllable degree of freedom is added, the optimal margin of the converter is increased, so the soft-switching range is widened, and the current stress, reactive power and other performance are optimized. Ref. [48] analyzes the characteristics of the reactive power under different voltage conversion ratios based on EPS control. By reducing the reactive power, the loss of power devices and magnetic elements is reduced, and the efficiency of the converter is improved. However, when operating modes varying from Boost to Buck or Buck to Boost, the operating states of the

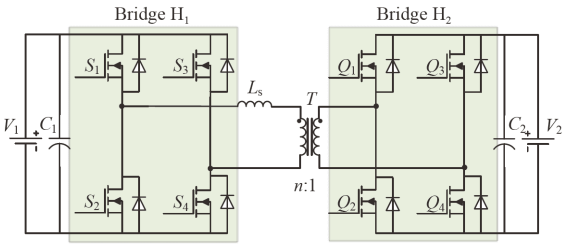

Figure 6 The circuit diagram of the DAB converter topology.

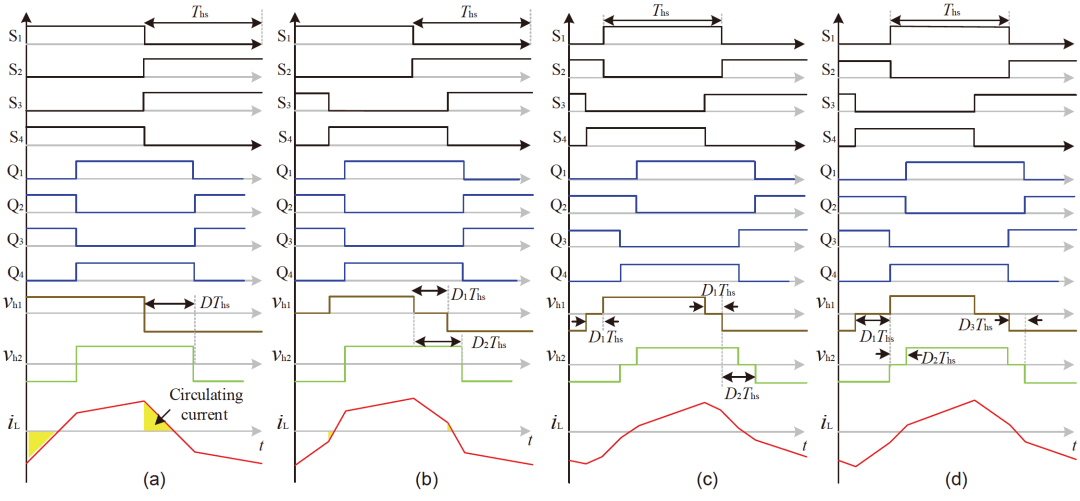

Figure 7 (Color online) Basic control methods of DAB. (a) SPS control; (b) EPS control; (c) DPS control; (d) TPS control.

primary H bridge and secondary H bridge need to be exchanged.

To solve this problem, the DPS control is proposed, in which there are same inner phase-shifts in both the primary H bridge and secondary H bridge as Figure 7(c) shown. Thus, both the output voltages are three-level waveforms. With this method, the operating states of primary H bridge and secondary H bridge do not need to exchange. The DPS can be implemented easily and owns better dynamic response. Ref. [49] proposes the minimum reactive power control based on dual DPS. The control strategy achieves the minimum reactive power control in the full power range by seeking the optimal shift ratio combination. The performance of EPS and DPS control is still not good under light load or extremely mismatched voltage operating conditions. To further increase the control degree, TPS control is proposed, in which the inner phase-shift in the primary H bridge and secondary H bridge are different as Figure 7(d) shown. Thus, there are three control degrees: D_1, D_2 and D_3. TPS is more complicated than the former three strategies, but has the best performance.

Besides using aforementioned control methods, the resonant tank is optimized to expand the soft-switching range of DAB derived converters. Ref. [50–56] proposes several typical resonant topologies based on DAB converter, as LC-type resonant topology, CLLC-type asymmetric resonant topology and new symmetric CLLC-type resonant topology, as shown in Figure 8. Compared with traditional DAB converters, these converters have the advantages of higher operating frequency and higher efficiency. From soft-switching performance, ZVS for primary-side switches and ZCS for secondary-side switches can be achieved in resonant topologies. In addition, LC-type DAB is easily controlled by phase-shift angle through phase-shift control, so the bidirectional transition speed of phase-shift control is faster. From soft-switching range, the CLLC-type resonant converter has wider soft-switching range than LC-type DAB, so it is more suitable for applications with wide voltage and power range. What's more, the CLLC-type asymmetric resonant converter shows different operations between forward and backward power flow directions compared to symmetric resonant converters.

Symmetric CLLC topology stands out because of its symmetrical typology and excellent switching condition [52], which is shown in Figure 8(c). Symmetric CLLC resonant converter can obtain soft-switching on both primary and secondary side when it operates at variable-frequency modulation. But the drawback of the modulation is the limited voltage regulating capacity.

To solve the problem of symmetric CLLC resonant converters, phase-shift modulation is gradually adopted. Extended phase-shift control is optimized in ref. [53] which helps to select the optimal and practical combination of inner

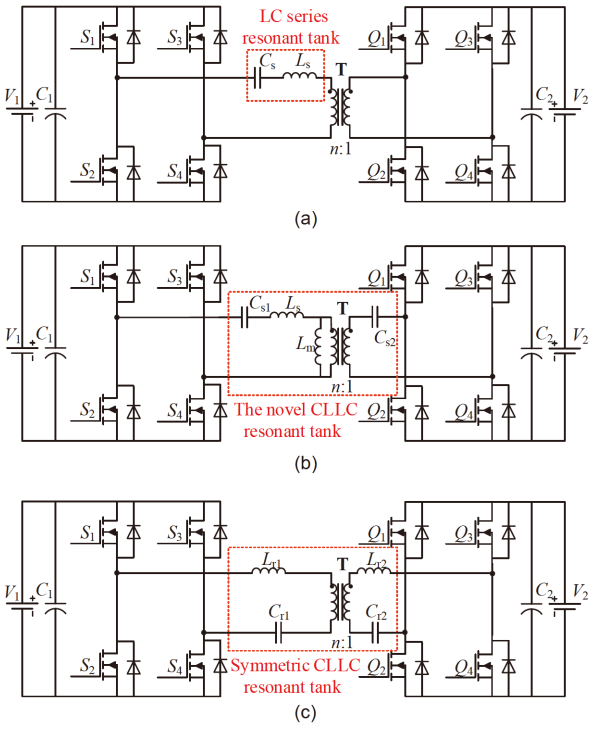

Figure 8 (Color online) Several typical resonant topology based on DAB converter. (a) LC-type resonant DAB; (b) CLLC-type asymmetric resonant DAB; (c) CLLC-type symmetric resonant DAB

and outer phase-shifts. Based on comprehensive calculation, it is concluded that when the outer phase-shift equals the half of the inner phase-shift, the full-bridge CLLC converter achieves maximum efficiency using EPS control. The optimization of EPS can improve the light load efficiency of full bridge CLLC resonant converter. The dual-phase-shift modulation is adopted in CLLC converter in ref. [54]. Based on the control method, dynamic response with load stepping up and down is stable and rapid. Also, the voltage gain is independent of the load and soft-switching of all the power switches can be achieved. In ref. [55], a synchronous rectification scheme based on small phase shift technique is proposed. Based the control method, the reactive current of low-voltage side can be eliminated when the switching frequency equals the resonant one, which can achieve a higher system efficiency and wider output voltage gain. Based on the similar idea, In ref. [56], a dual-control method is proposed for CLLC converter. Besides frequency modulation, phase shift between the primary and secondary switches is utilized as an additional control variable to effectively reduce the power loss and improve efficiency, especially in light- and medium-load conditions.

There is a tradeoff between safety (dead-time configuration avoiding shoot through) and dead-time loss. In order to achieve high efficiency, short dead time is expected. But long dead time is necessary to avoid shoot through failure, especially in light-load conditions. Because switches require

longer dead time in low turn-off current, it is harder to draw the charge out from the body diode and parasitic output capacitor to achieve ZVS. Ref. [57] proposes several adaptive dead-time control methods to solve the issue, but it would increase the converter complexity. With the development of wide band-gap semiconductor devices, such as GaN HEMT, the efficiency and power density of DAB converter can be improved significantly. Due to no reverse recovery performance, GaN HEMTs solve this issue and imply short dead-time and high efficiency power conversion.

Ref. [58] proposes an isolated bidirectional DC-DC converter replacing Si MOSFET with 650 V GaN HMET on the high voltage side. The circuit diagram is shown in Figure 9. The proposed theory is verified on a 1 kW, 100 kHz, 400 to 12 V DC-DC prototype converter which has a power density of 30 W/inch^3 and a peak efficiency of 98.3% in a wide input/output voltage range. Comparing with Si-based converter, about 1 W loss can be saved and the peak efficiency increases about 1.2% for the GaN HEMT-based converter.

In view of the above research status of DAB, the design and performance optimization of DAB based on WBG power devices will be the trend in future. Further key issues focus on the electrical optimization design methods of the topology, electrical parameters, and control strategy, to fully utilize characteristics of WBG power devices such as high temperature, high frequency, and low-loss, and the mechanical optimization design methods to further improve efficiency, power density, modularity and reliability.

2.3 Other resonant converters

In recent years, researchers have investigated on other resonant converter topologies. CLCL resonant topologies are proposed which are also suitable for high frequency applications with satisfactory soft switching characteristic [59–61]. The circuit is shown in Figure 10, with a resistive impedance of resonant tank, the switches can turn on in ZVS condition and turn off in ZCS condition under full load operating condition. Moreover, the diodes can also achieve ZCS turn-off. With the application of GaN switch and optimized planar magnetic components, the efficiency of the 1 MHz 20 W prototype is up to 90.9%.

Ref. [62] proposes a high-frequency and high-efficiency CLL resonant converter as an option for offline applications, as shown in Figure 11. This topology can realize ZVS from zero load to full load and ZCS of output rectifiers, making the realization of secondary rectification easier. An optimal design methodology is proposed to achieve high efficiency over a wide load range and an optimal transformer structure is introduced to achieve low winding loss. The proposed theory is verified on an 800 kHz, 250 W CLL resonant converter prototype, and over 96% efficiency is achieved for the wide load conditions. The proposed CLL resonant converter is an ideal choice for the next-generation of high-frequency, high-efficiency and high-power-density power supply.

LCLC resonant converters have the advantage of ZVS and ZCS, which are widely used in the electronic power conditioner in travelling-wave tube amplifiers. The circuit of LCLC converter is shown in Figure 12. Ref. [63] proposes a converter which can achieve load-independent output current by utilizing an LCLC resonant network, and realize high efficiency using a comprehensive design optimization methodology. By utilizing phase-shift control, the proposed LCLC resonant converter is also capable of regulating its output current at any desired value. The proposed theory is verified on a 2 MHz LCLC resonant converter which has an

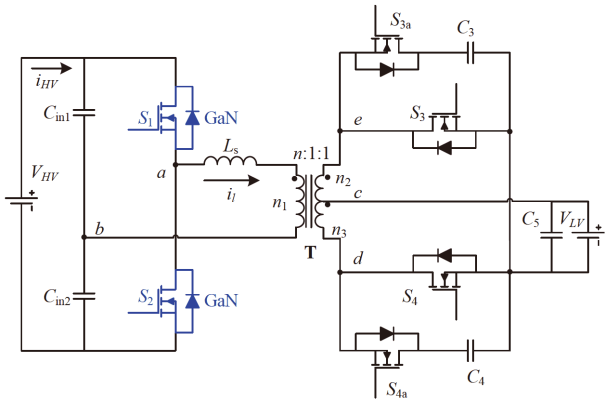

Figure 9 (Color online) Proposed topology based on GaN HEMTs.

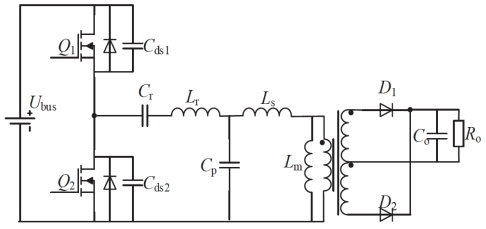

Figure 10 The circuit of CLCL converter.

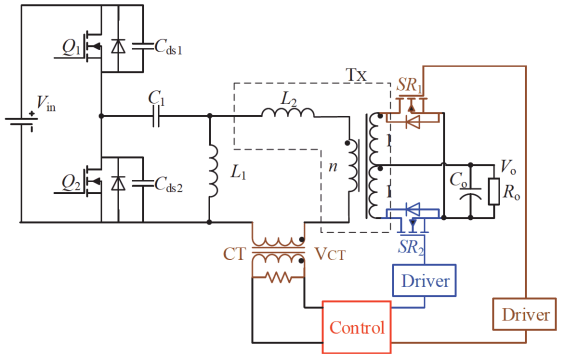

Figure 11 (Color online) CLL resonant converter with SR driving scheme.

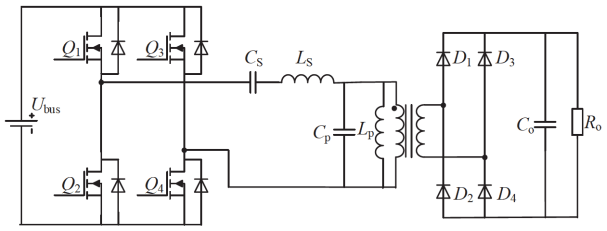

Figure 12 The circuit of LCLC converter.

input voltage of 14 V, an output voltage range of 3 to 50 V and a constant output current of 0.5 A. The LCLC resonant converter prototype achieves a peak power stage efficiency of 91.8% and maintains an average efficiency of 89.2% within its output voltage range.

Table 1 [43,58,62,64–67] shows the comparisons of the different high frequency resonant DC-DC power converters.

3 Planar magnetic components

In high frequency condition, the value of inductor and transformer can be greatly reduced. Thus, planar magnetic components are widely adopted which can reduce the profile and size of the magnetics, consequently improve the power density [14,15].

3.1 Winding structure model and design

The copper tracks on PCB are adopted as the windings of planar magnetic components, which owns good consistency, however, the winding is difficult to rearrange once PCB is manufactured. Thus, it is important to model the planar magnetic components. However, for the design of planar magnetics, many coupled factors greatly affect the properties of the inductors and transformers, such as copper track structure and winding layout. Though simulations can help to guide the design process, there is not a clear explanation about how these factors affect the magnetics properties. Some more effective ways should be adopted to help the planar magnetics design.

Response surface methodology (RSM) proposed in ref. [68] was adopted to design planar inductors considering factors such as copper thickness, track width, and track turns, which may be coupled and form a nonlinear relationship. The basic idea of RSM is to extract parameter models through regression analysis of the results obtained from several experiments and simulations. With the method, the inductance or resistance of the inductor can be represented by a function with previously chosen parameters as variables. Thus, the winding structure can be fast decided based on the function results.

For planar magnetics, besides inductors, planar transformers are also very important, especially those in the resonant DC-DC converters such as LLC circuit and DAB circuit, which play the role of high-ratio voltage transferring and isolating. Comparing with planar inductors, the structure of planar transformers is more complicated. For example, the turns in primary side and in secondary side have to be located in different PCB layers which causes many different layout choices, so it is hard to still use RSM to design transformers in different structure conditions.

Because there are many layers in the planar transformers and some relationships between them are formed, a modular layer model (MLM) based on lumped circuit is adopted in ref. [15]. In the design process, many factors affect the properties of planar transformers, such as winding layout, insulation materials, thickness of insulation layers, and copper thickness. The basic idea of MLM is to build a three-port model for each layer windings based on the electric field and magnetic field relationship, and then connect single layer model together by equivalent impedance as Figure 13 shown. For the obtained model, it can be transferred to typical T model by short-circuit test and open-circuit test with simulation.

As the RSM and MLM showing, they can provide systematic modeling method for magnetic inductor and transformer, which can reduce the design time by time-consuming simulation method. However, it should be mentioned here that usually the FEA simulation should be conducted to obtain an exact result to help slightly adjust the final winding structure before manufacturing.

Table 1 Comparison of different high frequency converters

Topology	f_s	Input voltage	Output voltage	Output power	Isolation	Efficiency	Primary side switch state		Secondary side switch state	
							Turn on	Turn off	Turn on	Turn off
LLC [43]	1 MHz	380 V	12 V	800 W	Yes	97.6%	ZVS	Hard	Hard	ZCS
DAB [58]	100 kHz	400 V	12 V	1000 W	Yes	98.3%	ZVS	Hard	ZVS	Hard
CLL [62]	800 kHz	400 V	12 V	250 W	Yes	96%	ZVS	Hard	ZVS	Hard
LLC [64]	1 MHz	300 V	12 V	120 W	Yes	90%	ZVS	Hard	Hard	ZCS
LLC [65]	1 MHz	360 V	40 V	1000 W	Yes	96.5%	ZVS	Hard	Hard	ZCS
CLLC [66]	1 MHz	400 V	18–24 V	400 W	Yes	94.3%	ZVS	Hard	Hard	ZCS
LCLC [67]	500 kHz	40 V	4800 V	295W	Yes	96.8%	ZVS	ZCS	ZVS	ZCS

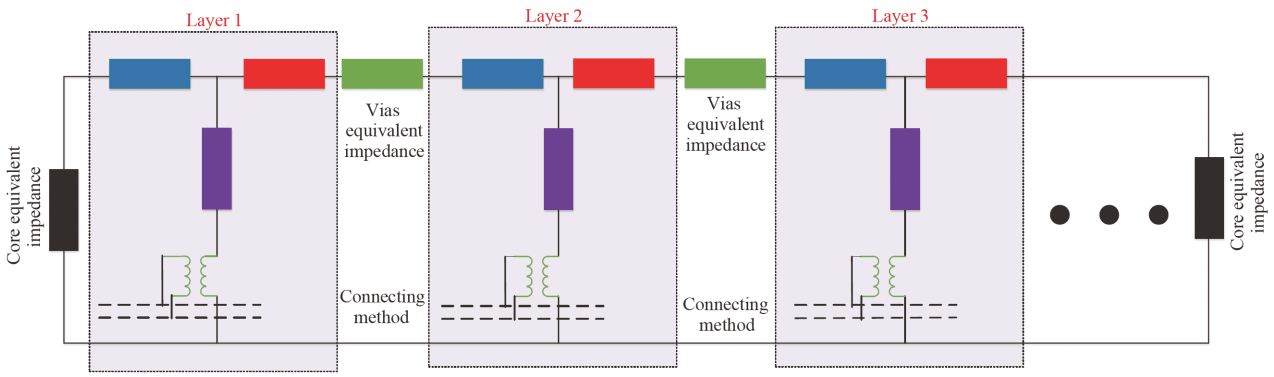

Figure 13 (Color online) General diagram of MLM of planar transformer.

Because of skin effect and proximity effect, the winding AC resistance increases rapidly under high frequency situations. In planar magnetic components, the width and thickness of winding can be adjusted flexibly.

To reduce the AC resistance, a variable width winding structure is adopted in ref. [69], and the winding structure is shown in Figure 14. The main idea of this winding structure is to achieve a constant track resistance for each turn, thus the width of turn geometrically change from inner turn to outer turn. In this structure, the most important factor is the radius ratio of adjacent windings. The minimum AC resistance is determined by the radius ratio and the number of turns per layer simultaneously.

For planar magnetic components, the AC resistance can be reduced by using interleaved structure which is very difficult to be adopted in traditional wounded magnetic components. For multilayers condition, AC resistance is affected by magneto-motive force (MMF). Figure 15 shows the MMF distribution of interleaving structure and non-interleaving structure. From the figure, it can be seen that the interleaving arrangement can realize a more even field strength and MMF distribution, which helps to achieve a smaller AC resistance.

However, there should be a compromise to determine the interleaving degree. A fully interleaving structure can help to reduce the winding AC loss and leakage inductance, however, lead to large parasitic capacitance caused by large facing area. On the other hand, a non-interleaving structure can greatly reduce capacitance, however, lead to large AC resistance and leakage inductance. Thus, there should be a priority among the AC resistance, leakage inductance and parasitic capacitance considering different application situations. Such as in a LLC circuit, usually the leakage inductance is expected to play the role of resonant inductor, thus, the leakage inductance should be increased by partial interleaving structure. There are also other methods to increase the leakage inductance, such as additional magnetic shunt method [70,71]. Similar to the leakage inductance, the parasitic capacitance can also be adopted as the resonant capacitor in high frequency DC-DC resonant circuit. Additional dielectric material can be put between different layers, and the corresponding capacitance can be adjusted by changing the material with different dielectric permittivity [72,73].

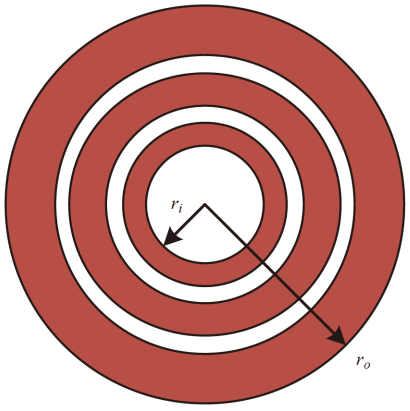

Figure 14 (Color online) Diagram of the ideal variable width spiral winding structure.

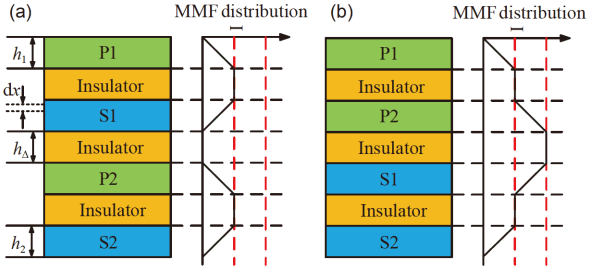

Figure 15 (Color online) Analytical scheme of MMF distribution of the transformer. (a) Interleaving structure; (b) non-interleaving structure.

However, in most situations of planar magnetic components, the small parasitic capacitance is needed, which can help to reduce the oscillation and EMI problem. Four methods can be used to reduce parasitic capacitance: (1) increase the distance between windings and reduce the surface area of overlapping as possible; (2) reduce the number of turns per layer and increase the number of layers within

cost range; (3) minimize the number of intersections between the primary and the secondary winding when designing the structure; (4) arrange winding connection reasonably to obtain minimum energy related to electric field [74,75].

3.2 Integration

Besides the copper loss, magnetic core loss also increases under high frequency condition. Thus, how to reduce the core loss is a main concern. Magnetic integration method is the most effective one to reduce core loss. Here takes planar matrix transformer proposed by CPES as an example to show the principle. Matrix transformer structure can help to increase the system voltage gain by stacking several transformers. However, using so many magnetic cores will not only increase the volume of the system but also increase the core loss. Thus, integration method for matrix transformer cores is the most effective method to reduce the core volume and loss.

Figure 16 shows one implementation of four core integration method for a matrix transformer structure [44]. Figure 16(a) shows the original structure formed by four sets of identical UI-cores. The primary winding winds one pillar of each core. The first two cores can be integrated into one based on flux cancellation principle, the same method can also be used for the last two cores, thus, the integrated two-core is shown in Figure 16(b).

From the structure of Figure 16(b), the two magnetic cores can also be placed from "horizontal" to "vertical" as Figure 16(c) shown; then it can be seen as a core with four pillars, where the flux of each pillar and magnetic plates are Φ_B. Another integration structure can be achieved by rotating 180 degrees of the second core in Figure 16(c). As Figure 16(d) shown, although the flux within the pillars remains the same, the flux density in the magnetic plates is reduced by half. This is very beneficial for high-frequency ferrite materials since the core loss is a considerable portion in the total loss and is mainly determined by the flux density.

4 Opportunities and challenges

Besides further development of topologies and planar magnetic components to achieve higher efficiency, higher power density and wider operating range, power device is also a very important research content field in the future. Because the device characteristics directly affect the operating mode of the DC-DC converter, the optimization of topology must take the device static and dynamic feature into consideration. In other words, for a certain device, a high performance converter should strengthen advantages and weaken disadvantages. For the future applications of high frequency resonant DC-DC converter, GaN FETs will be widely applied in low voltage and power situations and SiC MOSFETs will be widely applied in medium voltage and power situations. However, there are some intrinsic problems for these wide bandgap devices.

Dynamic resistance of GaN FETs is a serious problem which causes high conduction loss than expected. The dynamic resistance means that the on-resistance after turn-on immediately is significantly higher than its normal DC resistance value [18]. How to understand and measure the dynamic resistance are investigated recently. In the future work, besides the optimization of GaN devices to reduce dynamic, the suitable driving topology or method should also be studied to reduce the conduction loss.

Output capacitance loss of GaN and SiC devices is also a serious problem for the application of wide bandgap devices

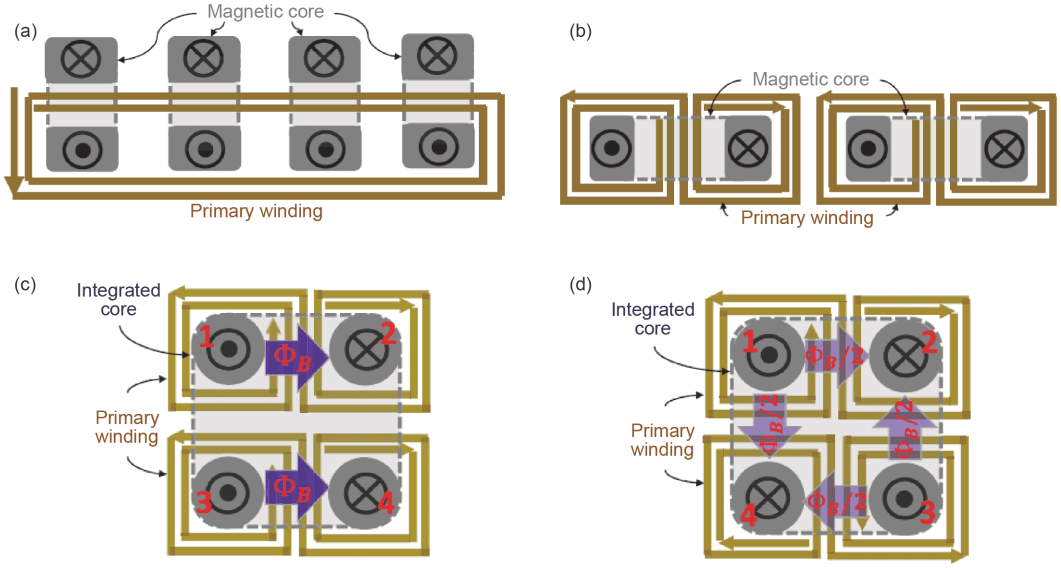

Figure 16 (Color online) (a) Separated structure; (b) half integration structure; (c) full integration structure 1; (d) full integration structure 2.

in high frequency resonant DC-DC converters [17,19]. The output capacitance loss phenomenon means that even the resonant DC-DC converter operates under soft-switching turn-off condition, there is still loss related with output capacitance, which is mainly considered to be caused by hysteresis characteristics. It greatly affects the performance of soft-switching power converters. The designers need to recalculate the total loss and loss distribution, and compromise the operation and the efficiency of soft-switching power converters operating in high frequency conditions. Also, with the increasing operating frequency, parasitic capacitive components of WBG components may be used as the resonant capacitor to resonate with planar magnetic component.

Meanwhile, because the GaN and SiC devices have high switching frequencies, parasitic parameters, especially the parasitic inductance will cause large voltage and current oscillations, resulting in higher power loss and serious EMI noise. Therefore, during the design of the driving circuit and power circuit, the corresponding parasitic parameters should be reduced through the optimized layout of the system components, especially the common source inductance (CSI) in half-bridge structure which is between the source and ground. In addition, the GaN FET has extremely low input and output capacitance, so its dv/dt and di/dt are generally 3 to 5 times than that of the Si switch during the switching process, which may cause the switch to be turned on or turned off by mistake.

Thus, to solve above problems better and further improve the frequency, the integrated module with power device and driving circuit should be developed. Some half-bridge modules have been developed, however, most of them are for low voltage situations. Such as LMG5200 manufactured by TI, the rated voltage is only 80 V. Thus, research on high voltage integrated module should be conducted. Also, with the development of integrated module or power IC, the device characteristics must be taken into consideration when the active and passive components integrated together.

5 Conclusion

With the development of high frequency resonant DC-DC power conversion technology, the system power density and efficiency can be greatly improved. For the system performance improvement, topologies and planar magnetic technologies play an important role. This reference firstly reviews the different resonant topologies, such as LLC circuit, DAB circuit, and other high order resonant circuit. The topology and control characteristics under high frequency conditions are described and compared. In Sect. 3, the characteristics of planar magnetic components are described, including the winding design, modeling and integration. Finally, the opportunities and challenges for high frequency resonant DC-DC converters are pointed out. This review can be a helpful guidance when designing high frequency resonant DC-DC converters.

This work was supported by the Research Start-Up Funding of HIT Young Talent Project.

1 Wu L, Xiao L, Zhao J, et al. Modelling and optimisation of planar matrix transformer for high frequency regulated LLC converter. IET Power Electron, 2020, 13: 516–524
2 Dao D, Lee D C, Phan Q D. High-efficiency SiC-based isolated three-port DC/DC converters for hybrid charging stations. IEEE Trans Power Electron, 2020, doi: 10.1109/TPEL.2020.2975124
3 Guan Y, Liu C, Wang Y, et al. Analytical derivation and design of 20 MHz DC/DC soft-switching resonant converter. IEEE Trans Ind Electron, 2020, doi: 10.1109/TIE.2020.2965508
4 Bai C, Han B, Kwon B H, et al. Highly efficient bidirectional series-resonant DC/DC converter over wide range of battery voltages. IEEE Trans Power Electron, 2020, 35: 3636–3650
5 Guan Y, Wang Y, Wang W, et al. A 20 MHz low-profile DC-DC converter with magnetic-free characteristics. IEEE Trans Ind Electron, 2020, 67: 1555–1567
6 Xu J Y, Xu P, Zhang Q, et al. The role of varied metal protrusions on the conductor surfaces in corona discharge subjected to DC high voltages. Sci China Tech Sci, 2018, 61: 1197–1206
7 Zheng K, Shen C, Liu F. Evaluation of commutation failure risk in single- or multi-infeed LCC-HVDC systems based on equivalent-fault method. Sci China Tech Sci, 2018, 61: 1207–1216
8 Li M B, Xiang W, Zuo W P, et al. The design and fault ride through control of un-interrupted DC-DC Autotransformer. Sci China Tech Sci, 2018, 61: 1935–1949
9 Li G, Wu X. High power density 48–12 V DCX with 3-D PCB winding transformer. IEEE Trans Power Electron, 2020, 35: 1189–1193
10 Li Y, Lyu X, Cao D, et al. A high efficiency resonant switched-capacitor converter for data center. In: Proceedings of the IEEE Energy Conversion Congress and Exposition (ECCE). Cincinnati, 2017. 4460–4466
11 Chung E, Lee K H, Han Y, et al. Single-switch high-frequency DC-DC converter using parasitic components. IEEE Trans Power Electron, 2017, 32: 3651–3661
12 Myers R H, Montgomery D C, Anderson-Cook C M. Response Surface Methodology: Process and Product Optimization Using Designed Experiments. New York: Wiley, 2016
13 Cove S R, Ordonez M, Luchino F, et al. Applying response surface methodology to small planar transformer winding design. IEEE Trans Ind Electron, 2013, 60: 483–493
14 Cove S R, Ordonez M. Wireless-power-transfer planar spiral winding design applying track width ratio. IEEE Trans Ind Applicat, 2015, 51: 2423–2433
15 Chen M, Araghchini M, Afridi K K, et al. A systematic approach to modeling impedances and current distribution in planar magnetics. IEEE Trans Power Electron, 2016, 31: 560–580
16 She X, Huang A Q, Lucia O, et al. Review of silicon carbide power devices and their applications. IEEE Trans Ind Electron, 2017, 64: 8193–8205
17 Guacci M, Heller M, Neumayr D, et al. On the origin of the C_{oss}-losses in soft-switching GaN-on-Si power HEMTs. IEEE J Emerg Sel Top Power Electron, 2019, 7: 679–694
18 Zulauf G, Guacci M, Kolar J W. Dynamic on-resistance in GaN-on-Si HEMTs: Origins, dependencies, and future characterization frameworks. IEEE Trans Power Electron, 2020, 35: 5581–5588
19 Tong Z, Zulauf G, Xu J, et al. Output capacitance loss characterization of silicon carbide schottky diodes. IEEE J Emerg Sel Top Power

Electron, 2019, 7: 865–878
20 Wang Y, Guan Y, Ren K, et al. A single-stage LED driver based on BCM boost circuit and LLC converter for street lighting system. IEEE Trans Ind Electron, 2015, 62: 5446–5457
21 Wang Y, Gao S, Guan Y, et al. A single-stage LED driver based on double LLC resonant tanks for automobile headlight with digital control. IEEE Trans Transp Electrific, 2016, 2: 357–368
22 Sun X, Shen Y, Zhu Y, et al. Interleaved boost-integrated *LLC* resonant converter with fixed-frequency PWM control for renewable energy generation applications. IEEE Trans Power Electron, 2015, 30: 4312–4326
23 Feng W Y, Lee F C, Mattavelli P. Optimal trajectory control of LLC resonant converters for LED PWM dimming. IEEE Trans Power Electron, 2014, 29: 979–987
24 Zhang W, Wang F, Costinett D J, et al. Investigation of gallium nitride devices in high-frequency LLC resonant converters. IEEE Trans Power Electron, 2017, 32: 571–583
25 Ren R, Liu B, Jones E A, et al. Accurate ZVS boundary in high switching frequency LLC converter. In: Proceedings of IEEE Energy Conversion Congress and Exposition (ECCE). Milwaukee, 2016. 1–6
26 Park H P, Jung J H. Power stage and feedback loop design for LLC resonant converter in high-switching-frequency operation. IEEE Trans Power Electron, 2017, 32: 7770–7782
27 Ta L A D, Dao N D, Lee D C. High-efficiency hybrid LLC resonant converter for on-board chargers of plug-in electric vehicles. IEEE Trans Power Electron, 2020, 35: 8324–8334
28 Jang Y, Jovanovic M M. Light-load efficiency optimization method. IEEE Trans Power Electron, 2010, 25: 67–74
29 Feng W, Lee F C, Mattavelli P. Optimal trajectory control of burst mode for LLC resonant converter. IEEE Trans Power Electron, 2013, 28: 457–466
30 Feng W, Lee F C, Mattavelli P. Simplified optimal trajectory control (SOTC) for LLC resonant converters. IEEE Trans Power Electron, 2013, 28: 2415–2426
31 Fei C, Feng W, Lee F C, et al. State-trajectory control of LLC converter implemented by microcontroller. In: Proceedings of 2014 IEEE Applied Power Electronics Conference and Exposition. Fort Worth, 2014. 1045–1052
32 Fei C, Li Q, Lee F C. Digital implementation of light-load efficiency improvement for high-frequency LLC converters with simplified optimal trajectory control. IEEE J Emerg Sel Top Power Electron, 2018, 6: 1850–1859
33 Park H P, Jung J H. PWM and PFM hybrid control method for LLC resonant converters in high switching frequency operation. IEEE Trans Ind Electron, 2017, 64: 253–263
34 Fu D, Liu Y, Lee F C, et al. A novel driving scheme for synchronous rectifiers in *LLC* resonant converters. IEEE Trans Power Electron, 2009, 24: 1321–1329
35 Fei C, Li Q, Lee F C. Digital implementation of adaptive synchronous rectifier (SR) driving scheme for high-frequency LLC converters with microcontroller. IEEE Trans Power Electron, 2018, 33: 5351–5361
36 Wei G, Bai H, Szatmari-Voicu G, et al. A 10 kW 97%-efficiency LLC resonant DC/DC converter with wide range of output voltage for the battery chargers in Plug-in Hybrid Electric Vehicles. In: Proceedings of 2012 IEEE Transportation Electrification Conference and Expo (ITEC). Dearborn, 2012. 1–4
37 Xu M, Jing J, Zhan L, et al. Design methodology of LLC converters based on simplified mode analysis for wide output range. In: Proceedings of 2016 IEEE 25th International Symposium on Industrial Electronics (ISIE). Santa Clara, 2016. 465–470
38 Shang M, Wang H. A voltage quadrupler rectifier based pulsewidth modulated LLC converter with wide output range. IEEE Trans Ind Applicat, 2018, 54: 6159–6168
39 Yuen K F, Chai Y P, Li R T H. DC/DC Converter with an Integration of Phase-Shift and LLC for Wide Output Voltage Range. In: Proceedings of 2018 IEEE International Power Electronics and Application Conference and Exposition (PEAC). Shenzhen, 2018. 1–6
40 Wolfspeed. 20 kW two-level AFE and 20 kW DC/DC for off-board charger. Datasheet. 2017. http://wolfspeed.com/media/wysiwyg/20kW_Two-level_AFE_and_20kW_DC_to_DC_for_Off-Board_-Charger_Demo_Summary_May_2018.pdf
41 Ngo K D T, Alpizar E, Watson J K. Modeling of losses in a sandwiched-winding matrix transformer. IEEE Trans Power Electron, 1995, 10: 427–434
42 Reusch D, Lee F C. High frequency bus converter with low loss integrated matrix transformer. In: Proceedings of 27th Annual IEEE Applied Power Electronics Conference and Exposition (APEC). Orlando, 2012. 1392–1397
43 Mu M, Lee F. Design and optimization of a 380 V–12 V high-frequency, high-current LLC converter with GaN devices and planar matrix transformers. IEEE J Emerg Sel Top Power Electron, 2016, 1
44 Fei C, Lee F C, Li Q. High-efficiency high-power-density LLC converter with an integrated planar matrix transformer for high-output current applications. IEEE Trans Ind Electron, 2017, 64: 9072–9082
45 Vazquez S, Lukic S M, Galvan E, et al. Energy storage systems for transport and grid applications. IEEE Trans Ind Electron, 2010, 57: 3881–3895
46 Heydt G T. Future renewable electrical energy delivery and management systems: Energy reliability assessment of FREEDM systems. In: Proceedings of IEEE PES General Meeting. Providence, 2010. 1–4
47 Zhao B, Song Q, Liu W, et al. Overview of dual-active-bridge isolated bidirectional DC-DC converter for high-frequency-link power-conversion system. IEEE Trans Power Electron, 2014, 29: 4091–4106
48 Zhao B, Song Q, Liu W. Power characterization of isolated bidirectional dual-active-bridge DC-DC converter with dual-phase-shift control. IEEE Trans Power Electron, 2012, 27: 4172–4176
49 Zhao B, Yu Q, Sun W. Extended-phase-shift control of isolated bidirectional DC-DC converter for power distribution in microgrid. IEEE Trans Power Electron, 2012, 27: 4667–4680
50 Li X D, Bhat A K S. Analysis and design of high-frequency isolated dual-bridge series resonant dc/dc converter. IEEE Trans Power Electron, 2010, 25: 850–862
51 Jung J H, Kim H S, Ryu M H, et al. Design methodology of bidirectional CLLC resonant converter for high-frequency isolation of dc distribution systems. IEEE Trans Power Electron, 2013, 28: 1741–1755
52 Chen W, Rong P, Lu Z Y. Snubberless bidirectional DC-DC converter with new CLLC resonant tank featuring minimized switching loss. IEEE Trans Ind Electron, 2010, 57: 3075–3086
53 Zhu T, Zhuo F, Zhao F, et al. Optimization of extended phase-shift control for full-bridge CLLC resonant converter with improved light-load efficiency. IEEE Trans Power Electron, 2020, 35: 11129–11142
54 Hua W, Wu H, Yu Z, et al. A phase-shift modulation strategy for a bidirectional CLLC resonant converter. In: Proceedings of 2019 10th International Conference on Power Electronics and ECCE Asia (ICPE 2019 - ECCE Asia). Busan, 2019. 1–6
55 Gao Y, Sun K, Lin X, et al. A phase-shift-based synchronous rectification scheme for bi-directional high-step-down CLLC resonant converters. In: Proceedings of 2018 IEEE Applied Power Electronics Conference and Exposition (APEC). San Antonio, 2018. 1571–1576
56 Zhang Z, Khaligh A. Modelling and optimisation of a dual-control MHz-level CLLC converter with minimised power losses in battery charging applications. IET Power Electron, 2020, 13: 1575–1582
57 Li J, Chen Z, Shen Z, et al. An adaptive dead-time control scheme for high-switching-frequency dual-active-bridge converter. In: Proceedings of 2012 Twenty-Seventh Annual IEEE Applied Power Electronics Conference and Exposition (APEC). Orlando, 2012. 1355–1361
58 Xue F, Yu R, Huang A Q. A 98.3% efficient GaN isolated bidirectional DC-DC converter for DC microgrid energy storage system applications. IEEE Trans Ind Electron, 2017, 64: 9094–9103
59 Wang Y, Guan Y, Xu D, et al. A CLCL resonant DC/DC converter for two-stage LED driver system. IEEE Trans Ind Electron, 2016, 63: 2883–2891
60 Guan Y, Wang Y, Xu D, et al. A 1 MHz half-bridge resonant DC/DC

converter based on GaN FETs and planar magnetics. IEEE Trans Power Electron, 2017, 32: 2876–2891
61 Guan Y, Wang Y, Wang W, et al. A high-frequency CLCL converter based on leakage inductance and variable width winding planar magnetics. IEEE Trans Ind Electron, 2018, 65: 280–290
62 Huang D, Fu D, Lee F C, et al. High-frequency high-efficiency *CLL* resonant converters with synchronous rectifiers. IEEE Trans Ind Electron, 2011, 58: 3461–3470
63 Khatua M, Kumar A, Maksimović Z, et al. A high-frequency LCLC network based resonant DC-DC converter for automotive LED driver applications. In: Proceedings of 2018 IEEE 19th Workshop on Control and Modeling for Power Electronics (COMPEL). Padua, 2018. 1–7
64 de Groot H, Janssen E, Pagano R, et al. Design of a 1-MHz LLC resonant converter based on a DSP-driven SOI half-bridge power MOS module. IEEE Trans Power Electron, 2007, 22: 2307–2320
65 Wu X, Chen H, Qian Z. 1-MHz LLC resonant DC transformer (DCX) with regulating capability. IEEE Trans Ind Electron, 2016, 63: 2904–2912
66 Wang Y F, Chen B, Hou Y, et al. Analysis and design of a 1-MHz bidirectional multi-CLLC resonant DC-DC converter with gan devices. IEEE Trans Ind Electron, 2020, 67: 1425–1434
67 Zhao B, Wang G, Hurley W G. *LCLC*. IEEE J Emerg Sel Top Power Electron, 2017, 5: 1272–1286
68 Cove S R, Ordonez M, Quaicoe J E. Modeling of planar transformer parasitics using design of experiment methodology. In: Proceedings of 2010 IEEE Canadian Conference of Electrical and Computer Engineering (CCECE). Calgary, 2010. 1–5
69 Guan Y, Wang Y, Wang W, et al. Analysis and design of a 1-MHz single-switch DC-DC converter with small winding resistance. IEEE Trans Ind Electron, 2018, 65: 7805–7817
70 Li M, Ouyang Z, Andersen M A E. *LLC*. IEEE Trans Power Electron, 2019, 34: 2405–2415
71 Perica G. Elimination of leakage effects related to the use of windings with fractions of turns. IEEE Trans Power Electron, 1986, 1: 39–47
72 Chen R, vanWyk J D, Wang S, et al. Improving the characteristics of integrated EMI filters by embedded conductive layers. IEEE Trans Power Electron, 2005, 20: 611–619
73 Fukuda Y, Inoue T, Mizoguchi T, et al. Planar inductor with ferrite layers for DC-DC converter. IEEE Trans Magn, 2003, 39: 2057–2061
74 Ouyang Z, Andersen M A E. Overview of planar magnetic technology—fundamental properties. IEEE Trans Power Electron, 2014, 29: 4888–4900
75 Zhao B, Ouyang Z, Duffy M C, et al. An improved partially interleaved transformer structure for high-voltage high-frequency multiple-output applications. IEEE Trans Ind Electron, 2019, 66: 2691–2702